BRUCE L. GOTWOLS and GEOFFREY B. IRANI

OPTICAL MEASUREMENT OF THE PHASE VELOCITY OF OCEAN WAVES DURING THE 1978 WAVE DYNAMICS EXPERIMENT

During the 1978 Wave Dynamics Experiment conducted by APL personnel, the phase velocity of wind-driven gravity waves was measured using a novel optical technique. Two observing sessions have been analyzed that are representative of low and moderate wind conditions. The observations agreed with linear theory to within 12%.

INTRODUCTION

The general aim of the Wave Dynamics Experiment conducted by APL personnel in 1978 was to study the dynamics of wind-driven gravity waves on the ocean surface. Gravity waves are given this name because gravity is the predominant restoring force that controls their oscillations. Familiar to any ocean bather, these are the waves a surfer rides and children play in at the beach. However, these coastline waves, known as shallow-water gravity waves, are critically dependent on the water depth, whereas the deep-water gravity waves we studied are independent of depth. (The transition from shallow- to deep-water gravity waves occurs when the water depth is approximately one half a wavelength.) Gravity waves occur with periods ranging from about 1000 to 0.1 seconds. Their wavelengths cannot be specified independently but are related to their frequency through an expression known as the dispersion relation. The corresponding wavelengths extend from 1600 km to 1.6 cm, with longer wavelengths corresponding to longer periods.

The primary goal of the Wave Dynamics Experiment was to determine the phase velocity of wind-driven gravity waves (Fig. 1). An accurate knowledge of wave phase velocity is necessary for progress in wind-wave theory and is extremely important in order to relate the new types of remote sensing data taken at many points simultaneously, to the conventional time series measurements at a single point. We were particularly stimulated by a controversy that

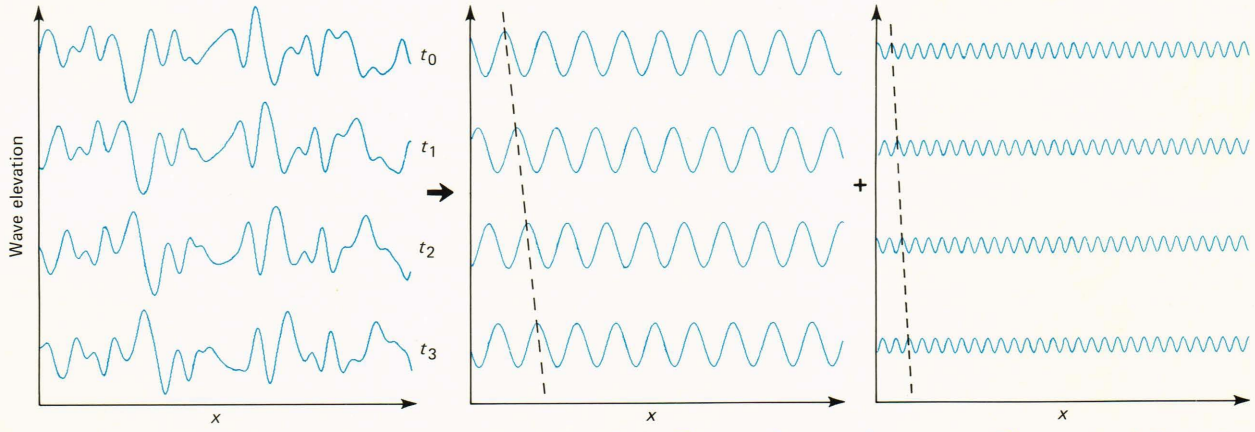

Fig 1—Modern wave theory relies heavily on Fourier analysis. Thus, at time t_0, the wave profile at upper left can be decomposed into a sum of sinusoids, two of which are shown to its right. At subsequent times, each sinusoid has progressed a distance that depends on its wavelength. The figure illustrates the classical theory of gravity wave propagation, where, as shown by the dashed lines, the speed of the sinusoid (phase velocity) is faster the greater the wavelength. Wave propagation such as this is said to be dispersive. As the complex waveform progresses toward greater x, the constituent sine waves combine to cause a constantly evolving wave profile.

arose during the past decade that questioned the validity, in the presence of sufficient wind, of the dispersion relation for deep-water gravity waves. That relation had been accepted with very little change for the past century. Because of the importance of the dispersion relation to wave theory, we conducted the Wave Dynamics Experiment, using a novel optical technique for obtaining phase velocity measurements of ocean wind waves in a more comprehensive fashion than had previously been attempted.

The phase velocity problem has an interesting background. By the beginning of the 19th century, it had been proposed that when a wave of sinusoidal form and infinitesimal amplitude propagates in an incompressible, zero viscosity fluid, the wave frequency, f, is related to the wavenumber, k, by the dispersion relation

$$f^2 = gk/2\pi .$$

Here g is the gravitational acceleration, $k = 1/\lambda$ is the wavenumber, and λ is the wavelength. According to this theory, the phase velocity is given by

$$c = f/k = \sqrt{g/2\pi k},$$

which shows that long waves travel faster than short waves, a fact easily verified by visual observation. In the mid-19th century, an important advance was made by Stokes,[1] who showed that, for a periodic wave of fixed profile and finite amplitude, the phase speed is at most about 10% greater than that of an infinitesimal amplitude wave of the same wavelength.

Theoretical contributions that follow Stokes' general approach have continued to the present day. However, virtually any observer of the ocean would agree that ocean waves bear little resemblance to waves of fixed profile traveling without change of form. There is a random aspect that is totally ignored by the Stokes model. Presumably stimulated by advances in the theory of random processes that occurred in the 1930's and 1940's, Pierson,[2] Phillips,[3] Longuet-Higgins,[4] and others began to develop a theoretical framework that recognized the random nature of ocean waves. The picture that emerged consisted of both wind generation and nonlinear interaction theories aimed at describing the slow evolution of a spectrum of waves. The phase speed associated with a given frequency component of a wind-wave spectrum was still thought to be approximately that predicted by Stokes.

The history of quantitative measurements of phase velocity is considerably shorter than its theoretical counterpart; experiment lagged well behind theory in the 19th century as a result of the complications inherent in obtaining continuous, synchronized records of waves at more than one point. Dating the onset of reliable measurements is difficult. Titov,[5] in the introduction to his book, mentions a number of experimental contributions starting in the 1930's but does not give detailed references. Some early measurements — conducted in 1938 and 1939 on mechanically generated waves — that agree with the small amplitude dispersion relation to within several percent are quoted by Defant.[6] However, owing to experimental results in the seventies by Soviet,[7] French,[8] and American[9] groups, a competing picture has recently emerged. It has been proposed that, for sufficiently steep wind waves, all Fourier components with frequencies above the frequency of the dominant energy-bearing component (dominant wave) propagate at the same speed as the dominant wave. The high-frequency components are thus bound wave components of the dominant wave. This concept is highly reminiscent of Stokes' model, but here components of random amplitude are included that are not necessarily integral harmonics of the dominant wave. Nonlinear interactions are strong in this model; hence, we will occasionally refer to this as nonlinear theory (even though all contemporary theories have an element of nonlinearity). This radical departure from the by now classical theoretical results is controversial and has been disputed by another group[10] in the field.

THE OPTICAL TECHNIQUE

Optical images have been used for many years to study ocean waves. The earliest quantitative work was done using stereo photography[11,12] that allowed simultaneous measurement of wave height over a large grid of points. However, very few stereo pair photographs have been analyzed because of the extremely tedious procedure. (With the tremendous increases in computing power that are occurring, this may no longer be an impediment.) A far simpler alternative was demonstrated qualitatively in the 1940's[13] and worked out quantitatively starting in the late 1960's.[14] When light from a uniformly illuminated sky is reflected from the ocean surface, the intensity recorded in the image plane is proportional to the reflection coefficient at the appropriate angle of incidence (Fig. 2). By carefully choosing the observing direction and polarization, the intensity will

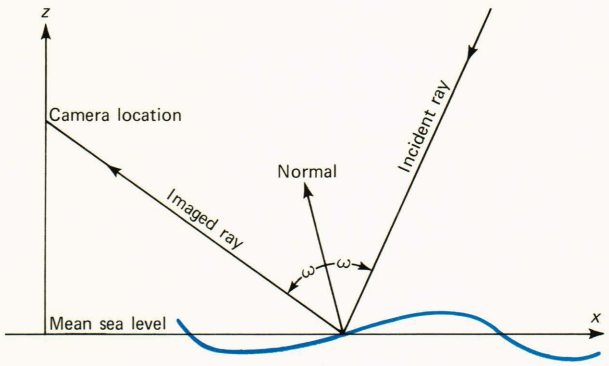

Fig. 2—Imaging geometry at the Stage I tower for the simplified two-dimensional case. An incident ray at incidence angle ω is reflected at the water surface and imaged in the focal plane of the video camera. Over a limited range of incidence angles, the reflection coefficient is approximately linearly proportional to wave slope; hence the wave slopes are encoded as intensity changes in the video image.

be approximately linearly proportional to one component of the wave slope. Nonuniform sky radiance tends to complicate this simple model, but the results are frequently still quite useful. A two-dimensional Fourier transform of such an image yields information on the two-dimensional directional wavenumber spectrum of the waves. For brevity both here and throughout the rest of the paper, we use the term "spectrum" to mean surface slope component spectrum. We extended this technique to the temporal domain by recording wave images rapidly in time. A three-dimensional Fourier transform of these data yields the so-called wavenumber-frequency spectrum from which the phase velocity is easily extracted.

CHOICE OF SENSOR

Film has traditionally been used to record wave images, but its successful use in analyzing wave spectra requires extraordinary care. On the other hand, video recording, because it operates in the electronic domain, offers the possibility of improved linearity and ease of use and is more readily converted to digital form. Conventional video sensors, however, suffer a phenomenon known as lag, which is the result of incomplete readout of a frame. This causes frame-to-frame smearing that constitutes an undesired filtering in the temporal frequency domain. These considerations prompted us to select a charge coupled device (CCD) sensor because of its excellent linearity, dynamic range, and absence of lag. There are, of course, some disadvantages — such as irregularities in the CCD response at various positions in the image and lower resolution than is possible with film — but the advantages have clearly outweighed the disadvantages.

A commercially available CCD camera (RCA TC1160 BE) with a resolution of 240 by 320 picture elements (pixels) forms the nucleus of the instrumentation developed at APL. Two steps were taken to improve the quantitative response of this camera. First, a synchronous rotating shutter was placed in front of the lens to eliminate the crosstalk between pixels that normally occurs in this frame-transfer type of CCD sensor because of the presence of the image on the chip during electronic readout. Second, all the camera's analog electronics were replaced with circuitry designed to provide a smooth roll-off at high frequency, in contrast to the unmodified camera's special edge enhancement circuitry, a feature that is undesirable in our application.

THE OBSERVATIONS

The observations were conducted over a period of six days in September 1978, from the Stage I tower[15] located in the Gulf of Mexico 19 km south of Panama City, Fla. The water depth of 30 meters at this site, in comparison to the wavelength of the longest waves observed, is such that no correction need be made to the dispersion relation for finite water depth. Each day was divided into morning and afternoon observing sessions. Midday observations were not conducted so that contamination of the images by sun glint could be avoided. As shown in Fig. 3, the CCD camera was located 25 meters above the water, observing at a depression angle of 30° and a focal length of 38 millimeters. Hence the region imaged was a trapezoid with the central dimensions given in Fig. 3. The camera was equipped with a horizontal polarizer and with a Kodak 25A red filter to minimize contamination from upwelling radiation that lies predominantly at the green end of the spectrum. (Only light reflected from the ocean surface is desired.) The images were recorded on a standard television cassette recorder, and, subsequently, back in the laboratory, carefully selected time sequences of 256 images covering a time span of 17.1 seconds each were digitized.

Supporting instrumentation consisted of a skyward-looking silicon camera equipped with a wide-

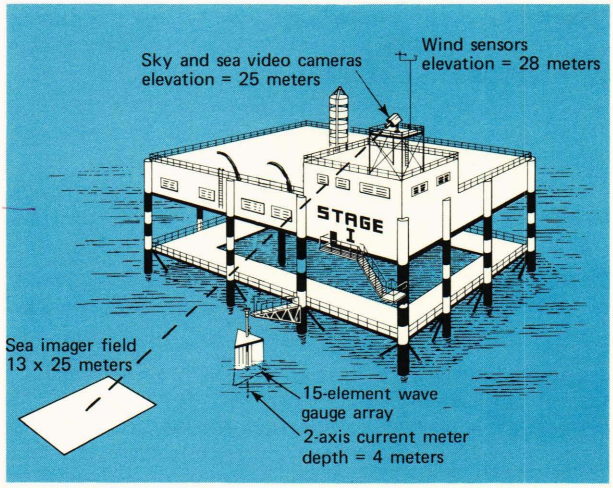

Fig. 3—The Stage I tower showing deployment of wave current and wind sensors. The field of measurement shown applies to data obtained on September 27, 1978, at 1604 hours CST. On September 26, the CCD camera was rotated 90° about the optic axis; hence its field of measurement was 30 meters along field by 10 meters across field.

angle lens for periodic recording of the sky radiance, an anemometer and direction vane for monitoring wind conditions, and a two-axis current meter for monitoring the net ocean current. A simultaneously operated 15-element array of wire wave probes that measure wave elevation by means of a capacitive technique has provided results that are consistent with the optical results reported below, albeit with much poorer wavenumber resolution and much better temporal frequency resolution.

THREE-DIMENSIONAL WAVENUMBER-FREQUENCY SPECTRUM

The main thrust of our analysis has been to calculate a three-dimensional wavenumber-frequency spectrum for each image sequence. Thus, if the waves propagated in accordance with linear theory, the power spectral density would be organized along a surface in k_x, k_y, f space, as shown in Fig. 4. Calculation of this spectrum requires careful preconditioning of the data because of the large gradient in signal caused by such factors as the increase in reflection coefficient with increasing angle of incidence, gradients in sky radiance, and, to a lesser extent, spatial variations in camera response. To effect these corrections, we first calculate a mean and standard deviation "picture" from the 256 images in the selected sequence. Each image is then corrected, on a pixel by pixel basis, by subtracting the mean and dividing by a spatially smoothed value of the standard deviation. Perspective distortion is then removed using linear interpolation techniques, and, finally, a cosine bell weighting factor is applied that minimizes the problem of discontinuities at the edges of the images. The Fast Fourier Transform algorithm is then used in each dimension to calculate the power spectral density for a cube of points consisting of 256 points on each side. (The Fast Fourier Transform is merely an efficient algorithm for calculating the Fourier transform that explicitly recognizes the discretely sampled nature of the data.)

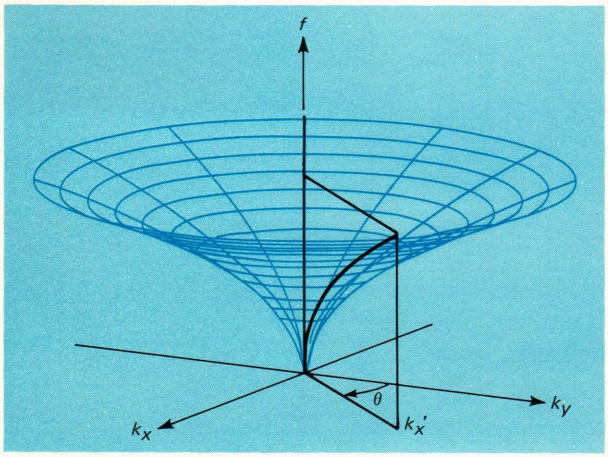

Fig. 4—Wavenumber-frequency (k-f) space. The funnel-like surface is associated with linear gravity waves:

$$f = \sqrt{gk}/2\pi.$$

Display of the power spectral density is facilitated by choosing a slice at angle θ (as shown) and plotting the values in pseudocolor.

One technique that has proved particularly useful for displaying these spectra is to plot a false color encoded image in the $k_{x'}$, f plane, as shown in Fig. 4. The $k_{x'}$ axis corresponds to wavenumber along a specified direction on the mean sea surface. Then, if linear wave theory prevails, one would expect to see the bulk of the power spectral density organized near the contour

$$f = \sqrt{g\,|k_{x'}|}/2\pi.$$

Another useful technique is to integrate over frequency from zero to infinity (in practice the integration is terminated at one-half of the sample frequency). This operation yields the (two-dimensional) wavenumber directional spectrum. Note that calculating the directional spectrum in this way does not result in the 180° directional ambiguity that one normally associates with an optical determination of the directional wavenumber spectrum. The physical reason for this fact is that we are dealing with a time sequence of images, and so it is possible to determine the specific direction of propagation, whereas, in the past, optically determined directional spectra have been based on a single image with the attendant 180° directional ambiguity.

IN SITU MEASUREMENTS

Data collected during two observing sessions on consecutive days have been selected for inclusion in this paper. Although wind and wave conditions were quite different for the two sessions, the phase velocity measurements were remarkably similar. However, before discussing the results of the video observations, it is useful to characterize the wind and wave conditions as measured with *in situ* sensors.

On September 26, 1978, the wind speed increased steadily for four hours, reaching a maximum just prior to the time of the video observations (Fig. 5). The average wind speed during the hour preceding the observations was 9.0 meters per second (m/s). The wind direction was approximately constant, generally coming out of the east. Over the same four hours and for perhaps another hour, the rms wave height increased continually, reached a plateau, and eventually declined. The elevation spectrum obtained from one element of our wave gauge array exhibits a dominant wave frequency of 0.33 hertz. From this we estimate the speed of the dominant wave to be approximately 5 m/s; thus, the wind was outrunning the dominant wave by almost a factor of two.

In contrast to the growing wind and wave conditions of September 26, on the next day the wind speed showed a gradual decline from 9.5 m/s in the morning to a 2.5 m/s average for the hour preceding our observations in the afternoon. The wind direction varied slowly during the day, generally coming

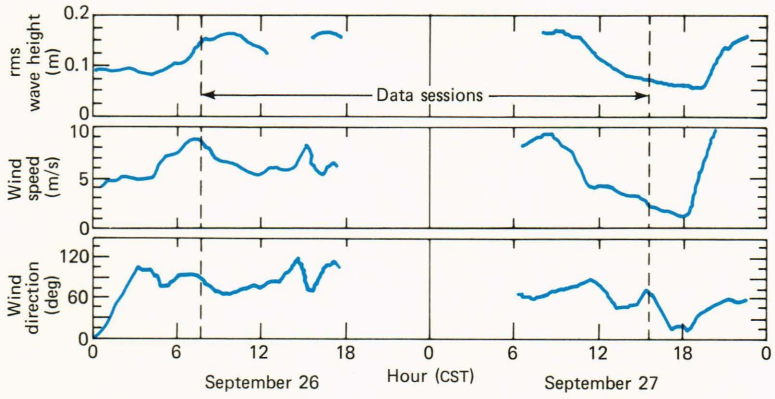

Fig. 5—Wind and wave data acquired at Stage I: September 26-27, 1978.

out of the northeast and east. Coincident with the decline in wind speed was a decline in rms wave height from 18 cm at 0800 hours to 8 cm at the time of the observations. The elevation spectrum shows a swell spectrum at 0.22 hertz and a dominant wave caused by local wind, with a peak at 0.45 hertz. An estimate of the speed of the wind-driven dominant wave yields a value of 3.6 m/s, which is greater than the 2.5 m/s wind speed.

Conditions on the two days provide a useful contrast. On September 26, the waves were growing and the wind was outrunning the dominant wave by a factor of approximately two; on September 27, the waves were decaying and the wind-driven dominant wave was outrunning the wind. By comparing these conditions with the published observations where bound wave behavior has been observed, we would expect that if significant nonlinear effects occur, they will appear in the September 26 data when the wind outran the waves, but not in the September 27 data when the reverse was true.

Sky conditions were not optimum on either day owing to heavy cloud cover with some patchiness. We believe the sky conditions will have a deleterious influence on the accuracy of the wavenumber directional spectrum but will not seriously corrupt our measurement of phase velocity because of the differential nature of this measurement.

RESULTS

Figure 6 summarizes the spectra calculated from the two data sequences discussed above. The two-dimensional directional wavenumber spectra (hereafter referred to as directional spectra) are shown on the left side of the figure. Because these spectra are obtained by integrating the three-dimensional spectrum over positive frequency, all that remains is the directional information. Thus the k_x and k_y axes are drawn horizontally and vertically, respectively. There is some disagreement in the optical and wave-gauge-array determination of this direction. The difference emanates from a distortion of the optically derived directional spectra caused by complicated gradients in the sky radiance. For this reason, we allowed results of the wave gauge array to determine the best direction for detailed analysis.

The directional spectra in Fig. 6 indicate that some waves propagate upwind, although the spectral densities in this direction are considerably lower than in the downwind direction. The complicated nature of the directional spectrum at the bottom left of Fig. 6 arises from both wave and sky conditions. On September 26, the waves were strongly driven and relatively well organized about the local wind direction; they dominated waves from other sources. On September 27, wave energy from the local wind was low, permitting waves from other sources to be more prominent, hence reducing the wave directionality. The patchy nature of the sky radiance on September 27 also contributed to the complexity of the directional spectrum on that day.

The right side of Fig. 6 displays a slice through the three-dimensional wavenumber-frequency spectrum

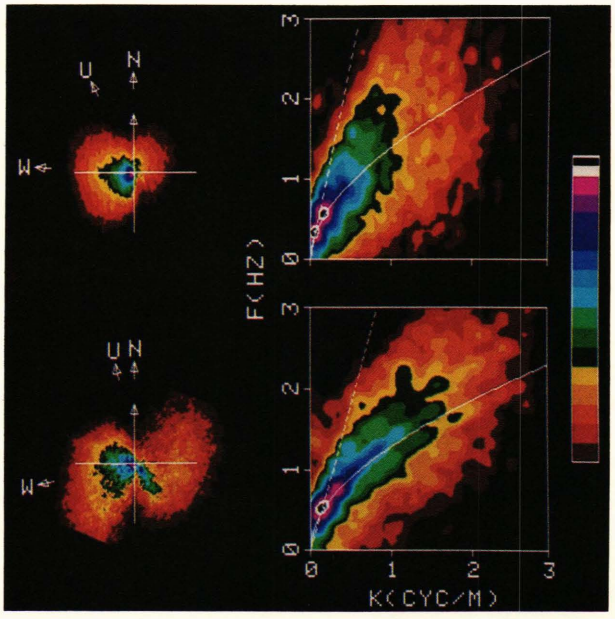

Fig. 6—Left side: directional wavenumber spectra. *W* is the wind vector, *U* is the current vector, and *N* is north. Right side: slices through the three-dimensional wavenumber-frequency spectra along the direction of the dominant wave (270° azimuth in both cases). All spectra in this figure have been normalized, logarithmically compressed over a 40 dB dynamic range, and encoded according to the color scheme shown on the extreme right.

for the two data sequences. In order to improve statistical stability, the spectrum was smoothed with an equally weighted three-dimensional weighting function consisting of three points on a side. The superimposed solid curves show the prediction of linear wave theory adjusted for current measured at the array. The straight dashed line is the dispersion relation of nonlinear theory where the high frequency waves propagate at the same speed as the dominant wave. Close inspection shows reasonable but not perfect agreement between linear theory and observation. The finite bandwidth tends to obscure the functional behavior of the observed spectra. To alleviate this problem, we developed a technique for quantifying the run of spectral density with wavenumber, by scanning the wavenumber frequency spectrum along the frequency axis and computing the centroid of the observed spectral values. The resulting "centroid frequencies" were then used to calculate a characteristic phase speed at each wavenumber. These phase speeds of both data sets follow linear theory rather well over the entire wavenumber range, albeit with a slight excess in velocity (Fig. 7).

Figure 8 shows these same data as a percent deviation from the prediction of linear theory. On September 26, the average deviation was 6%; on September 27, it was 12%. The greater deviation on September 27 is surprising in light of the low wind and wave conditions on that day. We have no explanation for this apparent inversion of the results from the expected. Perhaps it is more representative of some as yet undiscovered instrument bias rather than a true hydrodynamic effect.

We conclude that bound wave behavior is negligible in the two data sets analyzed, and linear gravity wave theory is adequate to describe our results to within ~12%. We are currently analyzing the remainder of our data in order to see if this trend continues. We are also conducting a collaborative experiment with the Naval Research Laboratory consisting of optical, probe, and microwave measurements of phase velocity in a wind-wave tank.

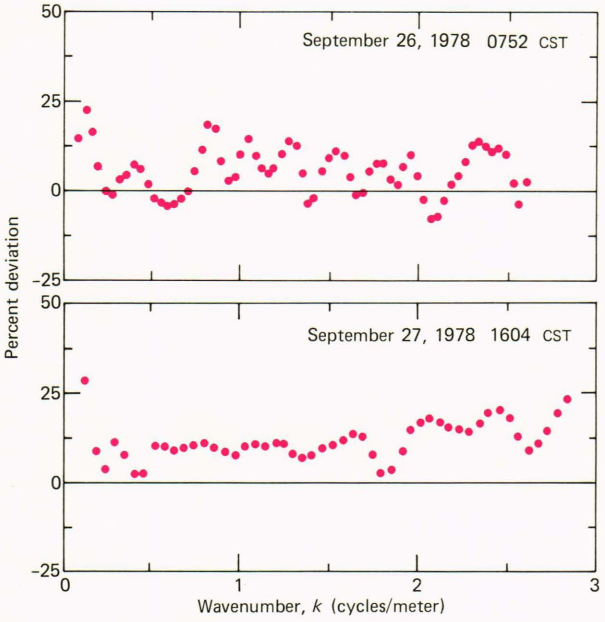

Fig. 8—Percent deviation of the measured phase speeds from the prediction of linear theory.

REFERENCES and NOTES

[1]G. Stokes, "On the Theory of Oscillatory Waves," *Trans. Camb. Philos. Soc.* **8**, pp. 441-455 (1847).

[2]W. J. Pierson, "Wind-Generated Gravity Waves," in *Advances in Geophysics* Vol. 2, pp. 93-178, Academic Press, New York (1955).

[3]O. M. Phillips, "On the Generation of Waves by Turbulent Wind," *J. Fluid Mech.* **2**, pp. 417-445 (1957).

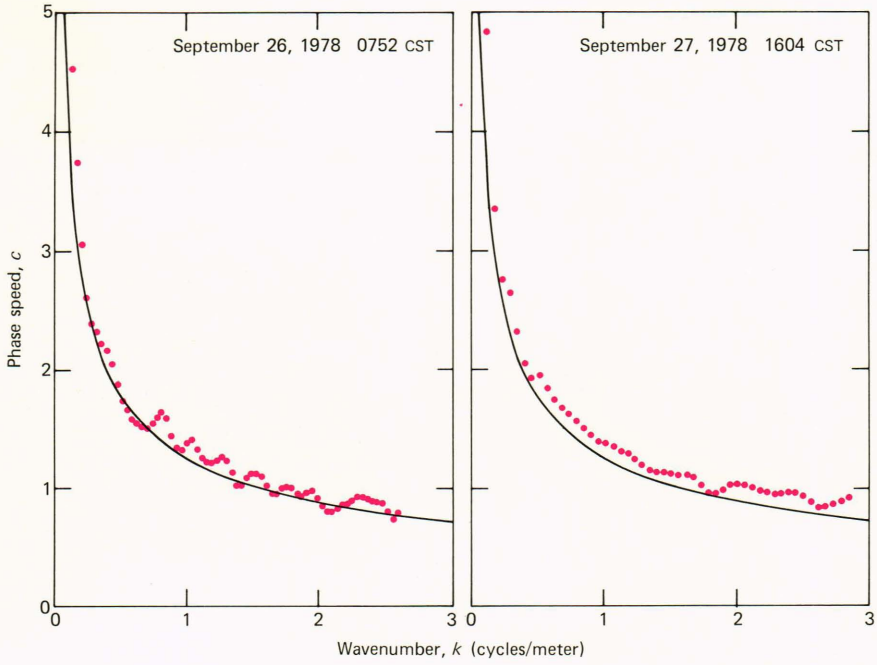

Fig. 7—Phase speed as a function of wavenumber for an azimuth in the direction of the dominant wind wave. The results from analysis of video data appear as circles and have been adjusted for advection by the measured current so that they can be compared with linear wave theory—the solid curve.

[4]M. S. Longuet-Higgins, "The Statistical Analysis of a Random Moving Surface," *Philos. Trans. R. Soc. London, Series A*, **249**, pp. 321-387 (1957).
[5]L. F. Titov, "Wind-Driven Waves," *Israel Program for Scientific Translations*, Jerusalem (1971).
[6]A. Defant, *Physical Oceanography*, Vol. 2, Pergamon Press, New York (1961).
[7]V. V. Yefimov, Y. U. P. Solov'yev, and G. N. Kristoforov, "Observational Determination of the Phase Velocities of Spectral Components of Wind Waves," *Izv. Acad. Sci. USSR, Atmos. Oceanic Phys.*, Engl. Transl. **8**, pp. 246-251 (1972).
[8]A. Ramamonjiarisoa and M. Coantic, "Loi Experimentale de Dispersion des Vagues Produites par le Vent une Faible Longueur d'Action," *C. R. Acad. Sci. Ser. B* **282**, pp. 111-114 (1976).
[9]B. M. Lake and H. C. Yuen, "A New Model for Nonlinear Wind Waves," *J. Fluid Mech.* **88**, pp. 33-62 (1978).
[10]W. J. Plant and J. W. Wright, "Spectral Decomposition of Short Gravity Wave Systems," *J. Phys. Oceanogr.* **9**, pp. 621-624 (1979).
[11]A. Schumacher, "Stereophotogrammetrische Wellenaufnahmen," *Wissenschaftliche Ergebnisse der Deutschen Atlantischen Expedition auf dem Forschungs - und Vermessungsschiff "Meteor", 1925-1927*, Vol. 7, text and atlas (1939).
[12]L. J. Cote, J. O. Davis, W. Marks, R. J. McGough, E. Mehr, W. J. Pierson, Jr., J. F. Ropek, G. Stephenson, and R. C. Vetter, "The Directional Spectrum of a Wind Generated Sea as Determined from Data Obtained by the Stereo Wave Observation Project," *Meteorol. Papers*, N.Y.U. College of Engineering, Vol. 2 (1960).
[13]N. F. Barber, "A Diffraction Analysis of a Photograph of the Sea," *Nature* **164**, p. 485 (1949).
[14]D. Stilwell, "Directional Energy Spectra of the Sea from Photographs," *J. Geophys. Res.* **74**, pp. 1974-1986 (1969).
[15]Stage I is an excellent platform for observing waves. The view is only slightly flawed by the occasional appearance of biological specimens. In other words, the fishing is excellent!

ACKNOWLEDGMENTS—J. Phipps, C. Richards, and A. Santos designed and constructed the special modifications to the RCA charge coupled device camera and integrated it into a coherent system. J. Rowland contributed valuable advice on video techniques throughout the experiment. D. Bullis made a number of important improvements to both the optical mount and the laboratory equipment. A. Bjerkaas generously provided results from the wave gauge array. R. Clark, J. Mashbaum, and B. Morgan wrote most of the computer programs and in the process overcame a number of difficult problems that resulted from the very large size of the computational task. D. Tilley used the Matrix camera of the Instrumentation Development Group to provide a high quality print of Fig. 6.